Gene mapping and preliminary functional validation of leaf spot resistance genes in barley (Hordeum vulgare L.)

Ruibin Ren
Gansu Agricultural University
Erjing Si
Gansu Agricultural University
Peiying Ye
Gansu Agricultural University
Guangyou Wan
Gansu Agricultural University
Dan Zhang
Gansu Agricultural University
Juncheng Wang
Gansu Agricultural University
Ganggang Guo
Chinese Academy of Agricultural Sciences
Hong Zhang
Gansu Agricultural University
Lirong Yao
Gansu Agricultural University
Xiaole Ma
Gansu Agricultural University
Baochun Li
Gansu Agricultural University
Huajun Wang
Gansu Agricultural University
Yaxiong Meng
yxmeng1@163.com
Gansu Agricultural University
Qijun Bao
Gansu Academy of Agricultural Sciences

Research Article

Keywords: Barley leaf spot, B. sorokiniana, Resistant identification, QTL, Resistant gene functional verification

Posted Date: July 31st, 2026

DOI: https://doi.org/10.21203/rs.3.rs-10368781/v1

Additional Declarations: No competing interests reported.

Abstract

Barley leaf spot, caused by *Bipolaris sorokiniana*, severely threatens global barley production by compromising grain yield and quality. Identifying resistance genes is therefore vital for breeding resilient cultivars. In this study, we developed F_2 and F_6 recombinant inbred line (RIL) populations from a cross between the resistant Mengpimai 3 and susceptible Mengpimai 1. Genetic analysis of the F_2 population revealed a normal distribution of disease severity, indicating quantitative inheritance of resistance. Combining genotypic data with spray inoculation assays, we performed QTL mapping using SNP arrays. Two QTLs, *qSRH7-59* and *qSRH7-60*, were identified in the RIL population. Validation using newly developed KASP markers confirmed these results, with three markers showing over 70% selection efficiency for the resistant genotype, highlighting their utility in marker-assisted breeding. To refine the mapping interval, high-density SSR markers were developed for the *qSRH7-60* region. Subsequent linkage mapping identified two resistance loci, *qSRH7-7* and *qSRH7-8*, and pinpointed the candidate gene *HORVU7Hr1G017950*, a cytochrome P450 family member. RT-qPCR analysis showed significantly higher transcript levels of *HORVU7Hr1G017950* in the resistant parent post-inoculation. Furthermore, BSMV-VIGS-mediated silencing of this gene significantly reduced resistance to *B. sorokiniana*, confirming its functional role in the defense response. These findings establish *HORVU7Hr1G017950* as a key candidate gene, providing valuable molecular resources for enhancing barley leaf spot resistance.

Background

Barley (*Hordeum vulgare* L.) is the fourth most produced cereal crop worldwide, following maize, rice, and wheat (Cheng et al. 2026). Its cultivation spans diverse agroecological regions owing to its resilience to abiotic stresses, such as drought and soil salinity (Nabawy et al. 2025). However, despite this adaptability, barley productivity is frequently constrained by biotic threats, particularly spot blotch caused by the fungal pathogen *Cochliobolus sativus* (anamorph: *B. sorokiniana*), which can lead to substantial yield losses and reduced grain quality worldwide (Villa-Rodríguez et al. 2019). *B. sorokiniana* affects wheat, barley, and other small-grain cereals, causing spot blotch, common root rot, and leaf spot (Gupta et al. 2018). The pathogen can be seed-borne or initiate infections through the dispersal of air- and soil-borne conidia. As a hemi-biotroph, it begins with a biotrophic phase restricted to individual epidermal cells, followed by a necrotrophic phase that induces host cell apoptosis (Jagdish et al. 2002). Spot blotch, one of the most destructive foliar diseases of barley, can occur at all growth stages and results in yield losses of 15–30% in infested fields, with susceptible varieties experiencing reductions of up to 40–50% (Guo et al. 2019). Given the limitations of chemical control and the environmental associated with fungicide use, breeding for genetic resistance represents the most economically viable and environmentally sustainable strategy for managing *B. sorokiniana* infections. Thus, identifying novel resistance genes in barley and its wild relatives is essential to accelerate the development of durable resistant cultivars (Kidokoro et al. 2022).

QTL mapping has been instrumental in dissecting the genetic basis of disease resistance in barley (Yang et al. 2024). Biparental populations-particularly RILs and doubled haploids (DH) lines-have enabled the

identification of genomic regions associated with resistance to multiple pathogens (Guan et al. 2017). For example, several QTLs conferring resistance to leaf spot and Ramularia leaf spot have been reported, including *Res5* on chromosome 7H (conferring seedling resistance), and *Res6* and *Res7* on chromosomes 1H and 6H, respectively (Drader et al. 2009; Ishihara et al. 2014). However, limited recombination in biparental populations often results in broad QTL intervals, which hinders fine mapping and gene cloning. Therefore, to improve resolution and capture greater allelic diversity, advanced mapping populations such as nested association mapping and multiparent advanced generation intercross have been developed (Li et al. 2023).

Concurrent advances in molecular marker technologies have accelerated marker-assisted selection (MAS) (Baidyussen et al. 2024). While SSR markers have long been used for their codominance and polymorphism (Zhai et al. 2016), SNPs and KASP assays now offer higher throughput, lower cost, and greater scalability. Indeed, KASP markers are particularly valuable in breeding programs due to their robustness and ease of implementation (Semagn et al. 2014). Genome-wide association studies (GWAS) have further expanded the toolkit. Zhou and Steffenson (2013) identified three resistance-associated loci-Res-qtl-3H-11_10565, Res-qtl-1H-11_10764, and Res-qtl-7H-11_20162-highlighting the polygenic nature of resistance. In parallel, Bovill et al. (2010) mapped resistance QTLs on chromosomes 3H and 7H using RIL populations, underscoring the importance of multi-environment evaluations to account for genotype-by-environment interactions.

Despite progress in QTL detection and marker development, functional validation of candidate genes remains a critical bottleneck. Virus-induced gene silencing (VIGS) has emerged as an effective approach for rapid functional assessment, particularly in species with low transformation efficiency (Fan et al. 2019). In barley, the Barley stripe mosaic virus (BSMV)-based VIGS system has been successfully applied to silence putative resistance genes and confirm their roles in defense responses (Lee et al. 2012). The integration of VIGS with fine-mapping enables targeted validation of candidate genes within QTL regions, thereby accelerating gene discovery and breeding applications.

The future of barley improvement lies in integrating multi-omics approaches (e.g., genomics, transcriptomics, and proteomics) to elucidate the molecular mechanisms underlying host-pathogen interactions. Integrating GWAS with machine learning may enhance prediction accuracy for resistance traits (Liu et al. 2024), while CRISPR-Cas9-mediated genome editing enables the engineering of durable resistance through precise modification of susceptibility genes (Ali et al. 2022).

In this study, F_2 and RIL populations were derived from a cross between the resistant genotype Mengpimai 3 (MP3) and the susceptible genotype Mengpimai 1 (MP1). Initial genome-wide scanning of the RILs via SNP arrays resolved putative resistance QTLs, which were subsequently fine-mapped to a candidate gene using high-density SSR markers. Functional validation was achieved by integrating transcriptomic profiling with BSMV-VIGS silencing assays. Ultimately, this research identifies a novel resistance locus and provides essential genetic resources and molecular markers to facilitate marker-assisted selection for barley leaf spot resistance.

Results

Disease assessment and resistance evaluation in populations

At the three-leaf stage, both the F_2 (n = 219) populations and RIL (n = 194) lines were inoculated with *B. sorokiniana* by spray application. Disease severity was assessed 14 dpi. In the F_2 population, the distribution of individuals across disease grades 0 to 9 was 10, 23, 27, 26, 29, 32, 25, 17, 17, and 13, respectively (Fig. S1A). The RIL population exhibited a continuous and unimodal distribution, with 0, 1, 12, 46, 51, 45, 19, 12, 7, and 1 lines per grade (Fig. S1B). Both populations displayed low skewness and kurtosis (absolute values < 1.0), indicating that phenotypic variation in disease resistance approximated a normal distribution. This continuous and near-normal segregation pattern strongly suggests that resistance to *B. sorokiniana* in the studied genetic background is quantitatively inherited and likely governed by multiple genetic loci.

Genotyping based on SNP arrays GBTS was performed on the parental lines MP1 and MP3 and the 194 RIL individuals. The raw sequencing data per sample ranged from 0.709 to 3.160 Gb (mean: 1.660 Gb). After quality control, the high-quality clean reads amounted to 0.687–2.985 Gb (mean: 1.599 Gb), representing an average of 96.32% of the raw reads. Prior to filtering, sequence coverage ranged from 4.728 to 21.065 Mb (mean: 11.069 Mb). After filtering, the high-quality bases averaged 11.011 Mb (range: 4.703–20.959 Mb). Base quality was consistently high across all samples, with Q20 values exceeding 94.73% and Q30 values greater than 85.77% (Table S2). Alignment to the barley reference genome resulted in mapping rates greater than 97% for all lines.

The genomic distribution of all SNP markers is illustrated in Fig. 1. The chromosomal distribution of SNP loci (Fig. 1A) indicates uniform coverage across all seven barley chromosomes. Analysis of the parental lines MP1 and MP3 revealed minimal missing data (< 2.3%) and very low heterozygosity (< 1.5%), confirming the expected high homozygosity and genetic stability of these inbred genotypes (Table S3). Functional annotation revealed that the majority of SNPs were located in intergenic regions (68.09%), followed by intronic (7.65%), 2 Kb upstream (6.80%), 2 Kb downstream (5.58%), exonic (5.53%), 3'-UTR (2.96%), and 5'-UTR (2.32%) regions. Minor categories included flanking regions upstream and downstream of genes (0.70%), overlapping UTRs of adjacent genes (0.31%), splice sites (0.04%), and exonic regions spanning splice junctions (0.02%) (Fig. 1B).

A total of 170, 842 polymorphic SNP markers identified from sequencing data were subjected to a systematic quality control pipeline. This included verification of parental genotype consistency, removal of ambiguous base calls, assessment of marker completeness, exclusion of loci exhibiting segregation distortion and selection of SNPs located within predefined target genomic regions of interest. After stringent filtering, 2,184 high-quality SNPs were retained for downstream analysis, representing 1.28% of the initial polymorphic variants.

Sample filtering was performed in three sequential steps to ensure data integrity: (i) removal of individuals with marker completeness below 70%; (ii) exclusion of putative duplicate lines exhibiting > 95% genotype identity; and (iii) elimination of samples with excess heterozygosity inconsistent with the expected high homozygosity of an RIL population. Six RILs were excluded based on these criteria: individual M154, which showed high genotypic similarity to the paternal parent MP3, and lines M19, M50, M151, M163, and M120 exhibited high heterozygosity.

Genetic map construction and QTL mapping based on SNP arrays

The genetic linkage map of the RIL population consisted of 2,184 high-quality SNP markers (Table S4; Fig. 1C), distributed across the seven barley chromosomes: 1H (198 markers), 2H (763), 3H (407), 4H (272), 5H (237), 6H (59), and 7H (248). The total map length was 1,576.98 cM, with an average marker density of one SNP per 0.72 cM. Chromosome 2H was the most densely saturated (763 markers; 205.87 cM), yielding an average interval of 0.27 cM between adjacent markers. In contrast, chromosome 6H had the lowest marker density (59 markers; 167.93 cM), resulting in a larger average spacing of 2.85 cM. Notably, chromosome 3H was the longest, spanning 329.91 cM, with an average marker interval of 0.81 cM. The map exhibited good coverage and continuity across all chromosomes.

Interval mapping identified a single QTL on chromosome 7H, designated q*SRH7-59*, located between flanking markers SNP-13635562 and SNP-27673224. This QTL spans a physical interval of 13.64–27.67 Mb, corresponding to a genomic region of 14.03 Mb (Table 1, Table S5; Fig. 1D). Within this interval, three SNPs (chr7H_22554114, chr7H_23167374, chr7H_27673224) showed significant associations with the trait, with LOD scores ranging from 3.25 to 3.35 and phenotypic variance explained (PVE) values of 0.02–1.14%. A total of 311 annotated genes reside within this region.

Using composite interval mapping, an additional QTL, *qSRH7-60*, was identified on the same chromosome and flanked by markers SNP-22554114 and SNP-27673224. This locus covers a physical interval of 22.55–27.67 Mb (5.12 Mb in length; Table 1, Table S6; Fig. 1E). Four SNPs (chr7H_22554114, chr7H_23167374, chr7H_24657620, and chr7H_27673224) showed significant marker-trait associations, with LOD scores ranging from 3.25 to 3.53 and explaining 0.02–2.28% of the phenotypic variance. A total of 115 annotated genes reside within this interval. Notably, Physical position comparison revealed that *qSRH7-60* is nested within the broader *qSRH7-59* interval, suggesting a potential major locus for the trait on chromosome 7H.

Fine mapping

To facilitate the fine mapping of the QTL on chromosome 7H, the initial *qSRH7-60* interval (5.12 Mb), identified via composite interval mapping of SNP chip data, was expanded by 1 Mb on each flank to define a 7.12 Mb target region. Subsequently, a dense set of novel markers was developed to saturate this interval, thereby enhancing mapping resolution.

A total of 1388 SSR markers were screened for polymorphism between MP1 and MP3, and 155 SSR markers exhibited polymorphic alleles. Of these, 149 markers (96.1%) were reliably amplified and polymorphic in the RILs (n = 183) and were used for genotyping. The chromosomal distribution of the polymorphic markers was as follows: 1H (9), 2H (19), 3H (13), 4H (11), 5H (11), 6H (16), and 7H (70) (Table S7, Table S8), which were employed to genotype 183 RIL lines. Eighteen markers (12.1%) showed significant segregation distortion ($P < 0.05$), primarily clustered in the pericentromeric regions of 5H and 7H.

Four QTLs for leaf spot resistance were identified on chromosomes 4H and 7H in the RIL population (Fig. 1F). All QTLs exceeded the genome-wide significance threshold (LOD ≥ 3.33) and explained 7.39–11.27% of the phenotypic variation (PVE). The QTLs were mapped to distinct genetic intervals: *qSSH4-11* (flanked by GBM1482 and GMS089), *qSRH7-7* (flanked by Bmg228 and Bmg385), *qSRH7-8* (flanked by Bmg385 and Bmg240), and *qSSH7-9* (flanked by Bmg672 and Bmg670). The additive effects of the QTLs indicated differential contributions from the parental lines. *qSSH4-11* and *qSSH7-9* had negative additive effects (-0.32 and − 0.58), indicating that susceptibility alleles at these loci were contributed by the parent MP1. In contrast, *qSRH7-7* and *qSRH7-8* had positive additive effects (+ 0.71 and + 0.67), with resistance alleles contributed by the parent MP3 (Table 1). *qSRH7-7* was tightly linked to marker Bmg228 (0.5 cM). The physical interval between the flanking markers Bmg228 and Bmg385 on chromosome 7H spans 1013 kb (Morex v3), encompassing 56 predicted genes. This region is a prime candidate for gene cloning, and marker-assisted selection in barley breeding.

KASP marker-based genotyping

Within the *qSRH7-60* QTL region, 21 polymorphic SNPs were identified (Table S9). Of which 14 were successfully converted into KASP markers (66.67% conversion rate). Parental polymorphism screening revealed that only five-KASP_24407061, KASP_24047573, KASP_24405607, KASP_26541006, and KASP_27422629-showed clear allele discrimination and distinct clustering in fluorescence-based genotyping.

For the five polymorphic KASP markers, MP1 and MP3 were fixed for alternative alleles: at KASP_24407061 and KASP_26541006, MP1 carried allele 1 (FAM) and MP3 allele 2 (VIC); at KASP_24047573, KASP_24405607, and KASP_27422629, MP1 carried allele 2 (VIC) and MP3 allele 1 (FAM). These markers were used to genotype the 183 RILs.

Genotyping results showed clear clustering of homozygous and heterozygous genotypes, allowing accurate allele calling. After excluding heterozygous and undetermined lines, the concordance between marker genotype and leaf spot phenotype was assessed (Fig. 2). For KASP_24047573, KASP_24405607, and KASP_26541006, 73.25–78.57% of lines with the resistant genotype were phenotypically resistant, and 28.38–29.49% of lines with the susceptible genotype showed susceptibility. In contrast, KASP_27422629 and KASP_24407061 exhibited lower phenotypic concordance (38.51% and 24.72%, respectively), respectively), despite high frequencies of the resistant allele in the population. Notably, all

lines carrying the susceptible allele at KASP_24407061 were resistant. KASP_24047573, KASP_24405607, and KASP_26541006 showed consistent co-segregation with leaf spot resistance in the RIL population. These markers exhibited high polymorphism and reproducibility in genotyping assays.

Screening and identification of candidate genes

In the fine-mapped *qSRH7-7* region (1013 kb), 56 predicted genes were identified through genome annotation (Morex v3). RNA-seq analysis revealed that 18 of these genes were differentially expressed between resistant and susceptible lines (Table S11). Based on functional annotations-particularly those encoding disease resistance-related proteins-eight genes were prioritized as candidate resistance genes.

The integration of RT-qPCR and RNA-seq data revealed high consistency between the two transcriptomic approaches, thereby validating the robustness and accuracy of our transcriptome profiling. Notably, the expression of *Hv7H.17950* peaked at 3 hpi with the leaf spot pathogen, and subsequently declined gradually (Fig. 3). Functional annotation indicates that *Hv7H.17950* encodes a cytochrome P450 protein. well-documented roles of cytochrome P450 genes in plant defense responses (Chakraborty et al. 2023; Ameen et al. 2021; Pandian et al. 2020), *Hv7H.17950* is proposed as a high-confidence candidate gene conferring resistance to barley leaf spot.

The *Hv7H.17950* sequence was obtained from the barley reference genome (Morex v3, NCBI). Molecular cloning identified a 1548-bp open reading frame encoding a 515-amino-acid protein.

Functional validation of Hv7H.17950 in barley resistance to leaf spot using VIGS

To evaluate the role of *Hv7H.17950* in leaf spot resistance, a VIGS assay was performed using BSMV-based vectors. Plants of the resistant cultivar MP3 were mechanically inoculated with BSMV: PDS, BSMV: *Hv7H.17950*, or BSMV: γb (vector control) in separate groups. Systemic photobleaching was observed in newly emerged leaves of BSMV: PDS-inoculated plants at 12 days post-inoculation (dpi), confirming effective virus-induced gene silencing (Fig. 4A). All virus-inoculated plants, including those in the BSMV: *Hv7H.17950* and vector control groups, developed chlorosis and scattered white streaks, which are typical symptoms of BSMV infection. The RT-qPCR analysis showed no significant difference in *Hv7H.17950* expression between mock-treated plants and those inoculated with BSMV: PDS, indicating that PDS silencing did not affect *Hv7H.17950* levels. Crucially, *Hv7H.17950* transcript levels were significantly reduced in BSMV: *Hv7H.17950*-inoculated plants compared to those carrying the vector control (BSMV: γb) (Fig. 4B), confirming effective gene silencing.

To assess the role of *Hv7H.17950* in disease resistance, MP3 plants inoculated with BSMV vectors were challenged with the *B. sorokiniana* strain Z14487 at 14 days post-virus inoculation. As a susceptibility control, the sensitive cultivar MP1 was inoculated with Z14487 under identical conditions and developed

severe necrotic lesions (infection type 8) by 14 days post-inoculation, confirming effective pathogen infection and high virulence.

The expression dynamics of *Hv7H.17950* were analyzed at 0, 3, 6, 12, 24, and 72 hours post-challenge in MP3 plants inoculated with BSMV: *Hv7H.17950* or the vector control (BSMV:γb) (Fig. 4C). Compared to the vector control, *Hv7H.17950* transcript levels were consistently downregulated in BSMV: *Hv7H.17950*-inoculated plants after pathogen inoculation, with a mean silencing efficiency of 66.87% across all time points (Fig. 4D).

Phenotypic assessment revealed that plants inoculated with the vector control (BSMV:γb) exhibited a highly resistant response to Z14487, with small, restricted lesions (scale 1). In contrast, plants in which *Hv7H.17950* was silenced displayed markedly enhanced disease severity, characterized by extensive chlorosis, necrosis, and rapid lesion expansion. Disease ratings for silenced plants rated scale 6, representing a significant increase in susceptibility compared to the vector control (Fig. 4C). This indicates that silencing of *Hv7H.17950* compromises resistance to leaf spot disease.

These findings demonstrate that silencing of *Hv7H.17950* compromises resistance to leaf spot disease, indicating that it functions as a positive regulator of defense responses in barley.

Discussion

Barley leaf spot persistently threatens global production and grain quality. Exploiting disease resistance genes and developing resistant cultivars represents the most economically viable and effective strategy to address this challenge. The phenotypic evaluation of the F_2 population revealed a continuous frequency distribution for leaf spot disease severity, deviating significantly from the discrete segregation ratios characteristic of qualitative, monogenic inheritance. This unimodal distribution, accompanied by transgressive segregation where certain progeny exceeded the resistance or susceptibility levels of the parents, strongly suggests that the resistance in this barley germplasm is governed by a quantitative inheritance mechanism involving multiple genetic loci with additive or epistatic effects. These findings align with the complex genetic architecture frequently reported for non-race-specific resistance in barley. For instance, Gyawali et al. (2018) demonstrated that resistance to *B. sorokiniana* in diverse barley panels is predominantly controlled by minor-effect QTLs rather than single major genes, necessitating a quantitative analytical approach.

The integration of high-density SNP genotyping, particularly through next-generation sequencing-based platforms, has significantly enhanced QTL mapping resolution by providing genome-wide marker coverage and facilitating the identification of candidate genes within mapped intervals (Wang et al. 2015). This approach has enabled the mapping of novel genes and resistance loci in various crops. For example, a gene associated with maize kernel development was mapped using 7, 903 SNPs (Gao et al. 2020), and leaf spot resistance loci on barley chromosomes 5H and 7H were identified through analysis of 3, 072 SNP markers (Zheng et al. 2023). In this study, a high-density genetic map was constructed using 2, 184 polymorphic SNP markers, spanning 1, 576.98 cM. QTL analysis via IM and CIM revealed a

major resistance locus on the long arm of chromosome 7H. A broad interval from 13.64 to 27.67 Mb (14.03Mb) was identified based on IM, designated *qSRH7-59*. Notably, the locus refined to a narrower region of 22.55–27.67 Mb (5.12 Mb) using CIM, here designated *qSRH7-60*, which is fully nested within *qSRH7-59*. This substantial reduction in interval size-from 14.03 Mb to 5.12 Mb-demonstrates the enhanced mapping resolution achievable with high-density SNP markers when combined with advanced statistical methods, thereby facilitating candidate gene prioritization.

Previous mapping efforts utilizing SSR markers have laid the groundwork for understanding blotch resistance in barley, successfully delineating key loci such as *Rbs7* on chromosome 6H (Wang et al. 2019) and the net-blotch resistance QTLs *QRpt6*, *QRpts4*, and *QRpt7* across chromosomes 4H, 6H, and 7H (Grewal et al. 2008). To improve the resolution of the initial 5.12 Mb QTL interval on chromosome 7H, a high-density marker scan was conducted within this region in this study. This analysis revealed two major resistance locus, designated *qSRH7-7* and *qSRH7-8*. Notably, comparative mapping positioned *qSRH7-8* within the confidence interval of *qSRH7-7*, suggesting they may represent the same underlying locus or tightly linked alleles. The positive additive effects for both QTLs indicate that the resistance alleles are derived from the paternal parent MP3. Concurrently, two susceptibility loci, designated *qSSH4-11* and *qSSH7-9*, were identified, with negative effects implicating susceptibility alleles from the maternal parent MP1. The precise delineation of *qSRH7-7* not only validates the efficacy of high-density genotyping in resolving complex QTL clusters but also provides a critical target for marker-assisted pyramiding. Future breeding strategies should prioritize the introgression of the MP3-derived resistance haplotype while simultaneously selecting against the MP1-linked susceptibility alleles to achieve durable field resistance.

KASP markers provide a high-throughput, automated platform for SNP and indel genotyping, combining high accuracy, operational flexibility, and cost efficiency (Williams et al. 1999). Their utility in MAS has been widely demonstrated across cereal crops. For instance, Hiraga et al. (2001) developed two KASP markers tightly linked (within 1.3 cM) to a resistance gene against wheat streak mosaic virus, validating their effectiveness in screening resistant germplasm. Noctor et al. fine-mapped the stem rust resistance gene *SrH2* to a 1.8–2.3 Mb interval on chromosome 1A, flanked by KASP markers, and demonstrated the utility of KASP-12147 in MAS breeding programs (Noctor et al. 2012). The conversion of SNP loci associated with agronomic traits into KASP markers significantly facilitates the screening of germplasm resources and expands the scope of marker-assisted selection in barley improvement. Shen et al. employed two KASP markers to delineate a QTL conferring leaf rust resistance to a 3.8–7.1 cM distal region on chromosome 2H in barley (Shen et al. 2025). Furthermore, Dhakal et al. predicted the resistance gene *Rph15*, developed corresponding KASP markers for population validation, and confirmed *Rph15* as a durable resistance source against leaf rust (Dhakal et al. 2018). Collectively, these studies highlight the scalability, reproducibility, and practical value of KASP markers in accelerating resistance breeding and facilitating the deployment of favorable alleles in cereal improvement programs. In the present study, 18 SNPs within the *qSRH7-60* interval were converted to KASP markers for application in resistance breeding. clear polymorphism between parental lines and were used to genotype the 183-line RIL population. All five markers successfully distinguished homozygous resistant, homozygous

susceptible, and heterozygous genotypes, demonstrating their reliability for genotyping. Showed high marker-phenotype co-segregation rates of 78.57%, 77.27%, and 73.25%, respectively, indicating strong predictive accuracy for the resistant phenotype. In contrast, the remaining two markers exhibited lower accuracies (38.51% and 24.72%), likely due to recombination events between the marker and the causal locus. The high-performing markers correctly identified resistant lines in 66, 68, and 63 RILs, respectively, confirming their utility for MAS in leaf spot resistance breeding. These results highlight the value of KASP markers for precise germplasm genotyping and efficient selection. However, the moderate performance of some markers may reflect the polygenic nature of leaf spot resistance and the inherent variability associated with visual disease scoring based on reaction type assessments, which can be influenced by environmental conditions and developmental stage.

The identification of candidate resistance genes within QTL mapping intervals provides a valuable foundation for disease-resistant breeding programs. Current studies localize major barley net blotch resistance QTLs to chromosome 1H (*Rrs14*), 3H (*Rrs1/Rrs3/Rrs4*), 4H (*Rrs6/Rrs9*), 6H (*Rrs13*), and 7H short arm (*Rrs2*) (Gazala et al. 2021). Chromosome 7H harbors additional resistance loci: *Rpt4* (Williams et al. 1999), *HvPtr* series genes (*HvPtr17* showing cytochrome P450 monooxygenase homology flanking *Rpt*4 at 4.7 cM from AWBMA11) (Hiraga et al. 2001), QTLs between ABG395-Rrn2 (LOD 3.5) (Rehman et al. 2018) and a locus at 107.4 cM with marker-trait correlations ($P < 0.05$) Tan et al. identified four candidate genes linked to rice leaf blast resistance through integrated QTL mapping and transcriptome analysis, followed by functional annotation of differentially expressed genes (Tan et al. 2022). In this study, an integrated approach involving fine QTL mapping, RNA-seq, and RT-qPCR validation allowed us to pinpoint *HORVU7Hr1G017950* as a key gene conferring resistance to barley leaf spot. This gene was annotated as a member of the cytochrome P450 family, and its putative function aligns with earlier findings reported by Gazala et al. (2021). SMV-mediated VIGS provides a rapid and effective alternative for functional validation of candidate genes (Bruun-Rasmussen et al. 2007), making robust reverse genetics approaches not only feasible but essential, which were exemplified by the findings of Liao et al. (2023), who demonstrated that BSMV-VIGS-mediated silencing of *HvMON1* markedly reduced its transcript abundance and consequently compromised barley resistance to powdery mildew, indicating a positive regulatory role for *HvMON1* in defense. Similarly, Yu et al. (2023) reported that knockdown of *HvWRKY2* via BSMV-VIGS enhanced barley susceptibility, as reflected by a significant increase in haustorium formation frequency, thereby implicating *HvWRKY2* as a negative regulator of *HvCEBiP* that suppresses basal immunity. Furthermore, Zhu et al. (2023) showed that silencing of the wheat resistance genes *Pm12* and *Pm21* through BSMV-VIGS led to substantially enlarged disease lesions, confirming their critical positive contribution to resistance against wheat powdery mildew. phenotypic analysis revealed a shift from reaction scale 1 (highly resistant) to reaction scale 6 (moderately susceptible), accompanied by widespread necrosis and chlorosis. Collectively, these findings support a role for *Hv7H.17950* as a positive regulator of defense responses against leaf spot in barley, a conclusion consistent with previous studies (Liao et al. 2023; Zhu et al. 2023)

Through fine mapping, this study delineated a major QTL for barley leaf spot resistance to a well-defined physical interval and identified *Hv7H.17950*, encoding a cytochrome P450 enzyme, as a high-confidence

candidate gene. While VIGS provided strong functional support, definitive validation of *Hv7H.17950*'s role will require genetic null alleles. CRISPR/Cas9-mediated knockout of *Hv7H.17950* in susceptible backgrounds, coupled with phenotypic assessment of disease resistance, would establish its necessity in the defense response. Future efforts should focus on elucidating the biochemical function of this putative P450 protein, which may catalyze the synthesis of defense-related secondary metabolites. Given that plant immunity often involves multi-protein complexes, protein–protein interaction assays-such as yeast two-hybrid (Y2H) or co-immunoprecipitation followed by mass spectrometry (Co-IP/MS)-could uncover interacting partners and place *Hv7H.17950* within a broader regulatory network.

In conclusion, translating *Hv7H.17950* from a candidate gene into a deployable tool for barley improvement will require integrated functional genomics, biochemistry, and breeding approaches. The narrow physical interval containing *Hv7H.17950* also presents an opportunity for marker-assisted selection, facilitating the rapid introgression of this resistance locus into elite barley varieties. This study provides a critical foundation for leveraging this locus in the development of disease-resistant cultivars.

Methods

Plant materials and pathogen isolates

The mapping population consisted of 219 F_2 individuals derived from a cross between the leaf spot-susceptible parent MP1 and the resistant parent MP3, along with 194 RILs advanced from the F_2 to the F_6 generation via single-seed descent.

For inoculum preparation, two *B. sorokiniana* isolates (Z14483 and Z14487) were cultured on potato dextrose agar (PDA; 200 g/L potato infusion, 20 g/L anhydrous D-glucose, 17 g/L agar) at 28°C in the dark for 7 days to induce sporulation. Conidia were harvested by washing the plates with sterile 0.25% (v/v) Tween-20 solution and gently dislodging spores using a sterile inoculation loop. All plant germplasm and pathogen isolates used in this study were derived from our research group.

Population resistance assessment

Disease resistance assays were conducted in a greenhouse. F_2 individuals at the three-leaf stage were uniformly spray-inoculated with a conidial suspension of isolate Z14483 (approximately 1×10^4 conidia mL^{-1}). To ensure successful infection, inoculated plants were incubated in darkness at 22 ± 2℃ with > 90% relative humidity for 48 h, after which they were returned to standard light conditions. Disease severity was evaluated approximately 14 days post-inoculation (dpi) using a 0–9 scale adapted from Fetch et al. (1999).

Two independent inoculation trials were conducted following a unified protocol: one using *B. sorokiniana* isolate Z14483 on 194 barley RILs, and the other using isolate Z14487 on 183 RILs, with disease severity assessed in both. The final phenotypic value for each line was derived as the mean disease score across

these two independent trials. Throughout all trials, the resistant parent MP3 and susceptible parent MP1 served as controls.

Genotyping based on SNP arrays

Leaf samples from the barley parental lines MP1 and MP3, as well as 194 lines of the RIL population, were collected. Genomic DNA was extracted from 100 mg of fresh leaf tissue using a modified CTAB-based method (Mwando et al. 2022; Porebski et al. 1997). The quality of the extracted DNA was assessed by electrophoresis on a 1% agarose gel, and concentration was estimated from the band intensity. DNA purity was determined by measuring the A_{260}/A_{280} ratio using a P100/P100 + Ultra-Micro spectrophotometer (Pultton Technology, Inc., USA) with a 1 μL sample volume.

Genomic DNA including MP1, MP3 and the RIL population were submitted to MolBreeding Biotechnology (Hebei, China) for genotyping analysis. Genotyping-by-Target-Sequencing (GBTS) technology with a 40 K target panel was used for high-throughput sequencing. Raw sequencing reads were processed for quality control using fastp (version 0.20) with the following parameters: -n 10 -q 20 -u 40. This step removed reads meeting any of the following criteria: (i) containing adapter sequences; (ii) having more than 10% ambiguous bases (N); (iii) exhibiting over 40% bases with a Phred quality score (Q) ≤ 20. The resulting high-quality (clean) reads were aligned to the barley reference genome (*Hordeum vulgare* L., Barley gene v3, cultivar Morex) using BWA-MEM.

Genotyping based on SSR marker

A total of 1, 388 SSR primer pairs were screened for polymorphism between the parental lines. The primers were derived from our internal repository and designed based on sequences archived in the public Grain Genes 3.0 database (https://wheat.pw.usda.gov/GG3/). PCR reactions were performed in a final volume of 10 μL for SSR marker, containing of 2 μL template DNA (50 ng/μL), 0.5 μL of each forward and reverse primer (10 μM), 5 μL 2×Taq PCR Master Mix (containing Taq DNA polymerase, dNTPs, $MgCl_2$, and optimized buffer) (TIANGen Biotech, Beijing), and 2 μL ddH_2O. PCR thermal cycling profile consisted of an initial denaturation at 95°C for 5 min, followed by 10 touchdown cycles (94°C for 30 s, 65 – 55°C for 30 s with a decrease of 1°C per cycle, and 72°C for 45 s), then 25 amplification cycles (94°C for 30 s, 55°C for 30 s, and 72°C for 45 s), with a final extension at 72°C for 10 min.

For fine mapping, the entire panel of 1,388 primer pairs was employed to screen the 183 lines of the RIL population. Subsequently, only those pairs exhibiting distinct polymorphism between the parental lines were retained for comprehensive genotyping of all individuals within the population.

Genetic map construction using SNP arrays and SSR marker

Variant calling was performed using the Genome Analysis Toolkit (GATK) (McKenna et al. 2010) (version v3.5-0-g36282e4) on the aligned sequence data. The identified SNPs were functionally annotated using ANNOVAR. Subsequent genotype filtering was applied to exclude SNPs that met any of the following

criteria: (i) missing genotype data in either parent; (ii) erroneous base calls; (iii) low genotyping rate (< 20%); or (iv) significant segregation distortion ($P < 0.01$). High-quality SNPs within target genomic regions were retained for downstream analysis. A high-density genetic linkage map was then constructed using the filtered SNP markers.

Genomic DNA from individual plants was amplified using polymorphic SSR markers under the same PCR conditions and cycling program described in Section 2.2. The PCR products were separated by 8% non-denaturing polyacrylamide gel electrophoresis (PAGE), visualized by silver staining, and scored based on the following banding patterns: A (allele from MP3), B (allele from MP1), H (heterozygous), and * (missing data due to failed amplification or unscorable bands). QTL analysis and genetic linkage map construction were conducted using QTL IciMapping V4.2 (Li et al. 2008; Meng et al. 2015), with a logarithm of odds (LOD) threshold of 3.0 used to identify significant QTLs. For each significant QTL, the phenotypic variation explained (PVE) and additive effects were estimated.

KASP marker development and validation

KASP markers were developed for high-throughput genotyping of the target QTL region. Genomic DNA from the parental lines (MP1 and MP3) and the RIL population (n = 183) was used for KASP genotyping. SNP sequences within the *qSRH7-60* interval, previously identified through composite interval mapping, were selected for KASP primer design using the online tool WASP (http://bioinfo.biotec.or.th/WASP). The allele-specific primers were modified at their 5' ends with universal fluorescence-labeled tails (Deng et al. 2022): FAM-labeled tail (F1: 5’-GAAGGTGACCAAGTTCATGCT-3’) and VIC-labeled tail (F2: 5’-GAAGGTCGGAGTCAACGGATT-3’). The 5-μL PCR reaction system contained: 2.5 μL of 2× KASP Master Mix, 1.25 μL of primer mix (containing both allele-specific and common reverse primers), and 1.25 μL of genomic DNA template (50 ng/μL). Thermal cycling conditions followed the standard protocol described in Section 2.2. The newly developed KASP markers were first validated by assessing polymorphisms between the parental lines. Subsequently, they were used to genotype the entire RIL population and estimate the phenotypic effects associated with the target QTL.

Candidate gene identification and expression analysis

Genes located within the fine-mapped interval were annotated using the barley reference genome database (Barley gene v3, cultivar Morex). To identify potential candidate genes associated with resistance to barley leaf spot, gene annotations were cross-referenced with transcriptome data previously generated by our research group. Expression levels of candidate resistance genes were quantified by RT-qPCR. Leaf samples from the resistant cultivar MP3 were collected at multiple time points following inoculation with *B. sorokiniana* strain Z14487-namely 0 h, 3 h, 6 h, 12 h, 24 h, and 72 h post-inoculation (hpi). Total RNA was extracted using the RNA simple Total RNA Extraction Kit (TIANGen Biotech, Beijing, China) according to the manufacturer's instructions. RNA concentration and integrity were assessed using a P100/P100 + Ultra-Micro spectrophotometer (Pultton Technology, Inc., USA) and agarose gel electrophoresis. First-strand cDNA was synthesized from 2 μg of total RNA using the FastKing RT SuperMix Kit (TIANGen Biotech, Beijing, China) in a 20 μL reaction volume, following the

supplier's instructions. Gene-specific primers were designed using the Primer-BLAST (Ye et al. 2012) tool (https://www.ncbi.nlm.nih.gov/tools/primer-blast/) hosted by the National Center for Biotechnology Information (NCBI) to ensure amplification specificity. Quantitative real-time PCR (RT-qPCR) was performed on the QuantStudio™ 5 Real-Time PCR Instrument (Thermo Fisher Scientific, Waltham, MA, USA) using SuperReal PreMix (SYBR Green) (TIANGen Biotech, Beijing, China) in a final volume of 20 μL per reaction. Each reaction contained 10 μL of 2× SuperReal PreMix Plus, 0.4 μL of 50× ROX Reference Dye, 0.6 μM of each forward and reverse primer, and 1 μL of diluted cDNA template, with RNase-Free ddH_2O added to 20 μL. The thermal cycling program consisted of an initial denaturation at 95°C for 5 min, and a final melting curve analysis from 65°C to 95°C with continuous fluorescence acquisition. Relative gene expression levels were calculated using the $2^{-\Delta\Delta Ct}$ method (Livak and Schmittgen 2001), with primer specificity confirmed by melt curve analysis and amplification efficiency validated in accordance with the MIQE guidelines (Bustin et al. 2009).

Preliminary functional validation of Hv7H.17950 gene using BSMV-VIGS methodology

A gene fragment targeting *Hv7H.17950* for silencing (Table S1) was amplified from MP3 cDNA using gene-specific primers containing *Apa*I restriction sites and subsequently cloned into the BSMV γ vector using T4 DNA ligase (Holzberg et al. 2002), generating the recombinant construct BSMV: *Hv7H.17950*. Positive control (BSMV-α, BSMV-β, BSMV-PDS; 1:1:1), experimental group (BSMV-α, BSMV-β, BSMV-*Hv7H.17950*; 1:1:1), and empty vector control (BSMV-α, BSMV-β, BSMV-γb; 1:1:1) were mechanically inoculated leaves and newly emerged leaves exhibiting virus-induced crinkling phenotypes were harvested, homogenized in sterile phosphate-buffered saline (PBS, pH 7.4), and used to inoculate the first leaves of seven-day-old barley seedlings by gentle friction.

A mock-inoculated control, treated with PBS alone, was included to exclude confounding effects of mechanical wounding. Symptoms on infected barley leaves were monitored and photographed. Upon confirmation of photobleaching in the PDS-silenced control plants, silencing efficiency of *Hv7H.17950* was quantified by RT-qPCR across all treatment groups. Concurrently, spore suspensions of the *B. sorokiniana* strain Z14487 were inoculated onto VIGS-silenced and control barley plants, with MP1 (a susceptible cultivar) serving as the pathogenicity control, methods were adapted from Jensen et al. (2016). Leaf samples from the experimental and empty vector control groups were collected at 0, 3, 6, 12, 24, and 72 hpi for quantitative analysis of pathogen colonization dynamics.

Conclusion

This study systematically characterized the genetic basis of resistance to barley leaf spot caused by *Bipolaris sorokiniana*. Through QTL mapping using SNP arrays and KASP markers, two major resistance loci, *qSRH7-59* and *qSRH7-60*, were identified on chromosome 7H. The development of high-efficiency molecular markers offers practical tools for the rapid screening of resistant germplasm in breeding pipelines. By employing fine-mapping strategies with SSR markers, we narrowed down the candidate region and identified *HORVU7Hr1G017950* as the most likely gene responsible for resistance. Functional

assays, including RT-qPCR and BSMV-VIGS, confirmed that this cytochrome P450-encoding gene plays a pivotal role in the defense mechanism against the pathogen. These findings not only advance our understanding of the molecular mechanisms underlying leaf spot resistance but also provide a solid foundation for the molecular design and improvement of disease-resistant barley cultivars.

Abbreviations

Abbreviation
English Full Name
BSMV
Barley stripe mosaic virus
DH
Doubled haploid
GWAS
Genome-wide association study
KASP
Kompetitive allele specific PCR
MAS
Marker-assisted selection
QTL
Quantitative trait locus
RIL
Recombinant inbred line
RT-qPCR
Reverse transcription quantitative polymerase chain reaction
SNP
Single nucleotide polymorphism
SSR
Simple sequence repeats
VIGS
Virus-induced gene silencing

Declarations

Ethics approval and consent to participate

Not applicable.

Consent for publication

Not applicable.

Conflict of interest

The authors declare no competing interests.

Funding

This work was supported by the National Natural Science Foundation of China (32160460); National Barley and Green Barley Industry Technology System (CARS-05-02A-02); Gansu Modern Cold and Arid Characteristic Agricultural Wheat Industry Technology System (GSARS-07); and Gansu Provincial Nature Fund Key Project (24JRRA637).

Author Contribution

RR, ES, QB and YM: were involved in experimental design, formal analysis, supervision, data curation, and writing-review and editing. PY, GW and DZ contributed to investigation and data visualization. JW, GG, HZ, LY, XM, BL and HW provided methodology and supervision. All authors approved the submitted version.

Acknowledgments

Not applicable.

Availability of data and materials

The datasets used and/or analyzed during the current study are available from the corresponding author on reasonable request.

References

1. Ali Q, Yu C, Hussain A, Ali M, Ahmar S, Sohail MA, et al. Genome engineering technology for durable disease resistance: Recent progress and future outlooks for sustainable agriculture. Front Plant Sci. 2022;13:860281.
2. Ameen G, Solanki S, Sager-Bittara L, Richards J, Tamang P, Friesen TL, et al. Mutations in a barley cytochrome P450 gene enhances pathogen induced programmed cell death and cutin layer instability. PLoS Genet. 2021;17:e1009473.
3. Baidyussen A, Khassanova G, Utebayev M, Jatayev S, Kushanova R, Khalbayeva S, et al. Assessment of molecular markers and marker-assisted selection for drought tolerance in barley (*Hordeum*

vulgare L). J Integr Agric. 2024;23:20–38.

4. Bovill J, Lehmensiek A, Sutherland MW, Platz GJ, Usher T, Franckowiak J, et al. Mapping spot blotch resistance genes in four barley populations. Mol Breed. 2010;26:653–66.
5. Bruun-Rasmussen M, Madsen CT, Jessing S, Albrechtsen M. Stability of barley stripe mosaic virus-induced gene silencing in barley. Mol Plant Microbe Interact. 2007;20:1323–31.
6. Bustin SA, Benes V, Garson JA, Hellemans J, Huggett J, Kubista M, et al. The MIQE guidelines: minimum information for publication of quantitative Real-Time PCR experiments. Clin Chem. 2009;55:611–22.
7. Chakraborty P, Biswas A, Dey S, Bhattacharjee T, Chakrabarty S. Cytochrome P450 gene families: role in plant secondary metabolites production and plant defense. J Xenobiotics. 2023;13:402–23.
8. Cheng J, Pan R, Zhang W, He T, Li C. An ancient super allele of the *Vrs1* gene driving the recent success in modern barley improvement through optimising spike architecture. J Integr Agric. 2026;25:602–9.
9. Deng M, Long L, Cheng Y, Yao F, Guan F, Wang Y, et al. Mapping a stable adult-plant stripe rust resistance QTL on chromosome 6AL in Chinese wheat landrace Yibinzhuermai. Crop J. 2022;10:1111–9.
10. Dhakal S, Tan CT, Anderson V, Yu H, Fuentealba MP, Rudd JC, et al. Mapping and KASP marker development for wheat curl mite resistance in TAM 112 wheat using linkage and association analysis. Mol Breed. 2018;38:119.
11. Drader T, Johnson K, Brueggeman R, Kudrna D, Kleinhofs A. Genetic and physical mapping of a high recombination region on chromosome 7H (1) in barley. Theor Appl Genet. 2009;118:811–20.
12. Fan Y, Hou B, Su P, Wu H, Wang G, Kong L, et al. Application of virus-induced gene silencing for identification of FHB resistant genes. J Integr Agric. 2019;18:2183–92.
13. Fetch J, Thomas G, Steffenson BJ. Rating scales for assessing infection responses of barley infected with *Cochliobolus sativus*. Plant Dis. 1999;83:213–7.
14. Gao S, Zheng Z, Hu H, Jiang Y, Liu M, Stiller J, et al. Delineating a locus conferring *Fusarium* crown rot resistance on chromosome arm 1HL in barley by developing and analysing a large population derived from near isogenic lines. Crop J. 2020;8:1002–10.
15. Gazala A, Shyam S, Lauren S, Jonathan R, Prabin T. Mutations in a barley cytochrome P450 gene enhances pathogen induced programmed cell death and cutin layer instability. PLoS Genet. 2021;17:e1009473–1009473.
16. Grewal T, Rossnagel B, Pozniak C, Scoles G. Mapping quantitative trait loci associated with barley net blotch resistance. Theor Appl Genet. 2008;116:529–39.
17. Guan H, Ali F, Pan Q. Dissection of recombination attributes for multiple maize populations using a common SNP assay. Front Plant Sci. 2017;8:2063.
18. Guo H, Yao Q, Chen L, Wang F, Lang X, Pang Y, et al. Virulence and molecular diversity in the *Cochliobolus sativus* population causing barley spot blotch in China. Plant Dis. 2019;103:2252–62.

19. Gupta PK, Vasistha NK, Aggarwal R, Joshi AK, Biology of, editors. *sorokiniana* (syn. *Cochliobolus sativus*) in genomics era. J Plant Biochem Biot. 2018;27:123–138.
20. Gyawali S, Chao S, Vaish SS, Singh SP, Rehman S, Vishwakarma SR, et al. Genome wide association studies (GWAS) of spot blotch resistance at the seedling and the adult plant stages in a collection of spring barley. Mol Breed. 2018;38:62.
21. Hiraga S, Sasaki K, Ito H, Ohashi Y, Matsui H. A large family of class III plant peroxidases. Plant Cell Physiol. 2001;42:462–8.
22. Holzberg S, Brosio P, Gross C, Pogue GP. Barley stripe mosaic virus-induced gene silencing in a monocot plant. Plant J. 2002;30:315–27.
23. Ishihara A, Mizuno N, Islam RA, Doležel J, Endo TR, Nasuda S. Dissection of barley chromosomes 1H and 6H by the gametocidal system. Genes Genet Syst. 2014;89:203–14.
24. Jagdish K, Patrick S, Ralph H, Gregor L, Helmut B, Elke S, et al. Bipolaris sorokiniana, a cereal pathogen of global concern: cytological and molecular approaches towards better controldouble dagger. Mol Plant Pathol. 2002;3:185–95.
25. Jensen B, Lübeck PS, Jørgensen HJ. Clonostachys rosea reduces spot blotch in barley by inhibiting prepenetration growth and sporulation of *Bipolaris sorokiniana* without inducing resistance. Pest Manage Sci. 2016;72:2231–9.
26. Kidokoro S, Shinozaki K, Yamaguchi-Shinozaki K. Transcriptional regulatory network of plant cold-stress responses. Trends Plant Sci. 2022;27:922–35.
27. Lee WS, Hammond-Kosack KE, Kanyuka K. Barley stripe mosaic virus-mediated tools for investigating gene function in cereal plants and their pathogens: virus-induced gene silencing, host-mediated gene silencing, and virus-mediated overexpression of heterologous protein. Plant Physiol. 2012;160:582–90.
28. Li G, Zhou Y, Li H, Zhang Y. A multi-locus linear mixed model methodology for detecting small-effect QTLs for quantitative traits in MAGIC, NAM, and ROAM populations. Comput Struct Biotechnol J. 2023;21:2241–52.
29. Li H, Ribaut JM, Li Z, Wang J. Inclusive composite interval mapping (ICIM) for digenic epistasis of quantitative traits in biparental populations. Theor Appl Genet. 2008;116:243–60.
30. Liao W, Nielsen ME, Pedersen C, Xie W, Thordal-Christensen H. Barley endosomal MONENSIN SENSITIVITY1 is a target of the powdery mildew effector *CSEP0162* and plays a role in plant immunity. J Exp Bot. 2023;74:118–29.
31. Liu Q, Zuo SM, Peng S, Zhang H, Peng Y, Li W, et al. Development of machine learning methods for accurate prediction of plant disease resistance. Engineering. 2024;40:100–10.
32. Livak KJ, Schmittgen TD. Analysis of relative gene expression data using real-time quantitative PCR and the $2^{-\Delta\Delta CT}$ method. Methods. 2001;25:402–8. https://doi.org/10.1006/meth.2001.1262.
33. Mckenna A, Hanna M, Banks E, Sivachenko A, Cibulskis K, Kernytsky A, et al. The Genome Analysis Toolkit: a MapReduce framework for analyzing next-generation DNA sequencing data. Genome Res. 2010;20:1297–303.

34. Meng L, Li H, Zhang L, Wang J. QTL IciMapping: Integrated software for genetic linkage map construction and quantitative trait locus mapping in biparental populations. Crop J. 2015;3:269–83.
35. Mwando E, Han Y, Angessa T, Zhang XQ, Li C. Fine-mapping and characterisation of genes on barley (*Hordeum vulgare*) chromosome 2H for salinity stress tolerance during germination. Crop J. 2022;10:754–66.
36. Nabawy MH, Najeeb KM, Khalil HB, Soliman KA, Seoudy AE. Integrated phenotypic and molecular evaluation of powdery mildew resistance in egyptian barley: identification of resistance-associated markers. Plants-Basel. 2025;14:1231–1231.
37. Noctor G, Mhamdi A, Chaouch S, Han Y, Neukermans J, Marquez-Garcia B, et al. Glutathione in plants: an integrated overview. Plant Cell Environ. 2012;35:454–84.
38. Pandian BA, Sathishraj R, Djanaguiraman M, Prasad PV, Jugulam M. Role of cytochrome P450 enzymes in plant stress response. Antioxidants-Basel. 2020;9:454.
39. Porebski S, Bailey LG, Baum BR. Modification of a CTAB DNA extraction protocol for plants containing high polysaccharide and polyphenol components. Plant Mol Biol Rep. 1997;15:8–15.
40. Rehman HM, Nawaz MA, Shah ZH, Ludwig-Müller J, Chung G, Ahmad MQ, et al. Comparative genomic and transcriptomic analyses of Family-1 UDP glycosyltransferase in three *Brassica* species and *Arabidopsis* indicates stress-responsive regulation. Sci rep. 2018;8:1875.
41. Semagn K, Babu R, Hearne S, Olsen M. Single nucleotide polymorphism genotyping using Kompetitive Allele Specific PCR (KASP): overview of the technology and its application in crop improvement. Mol Breed. 2014;33:1–14.
42. Shen B, Shen A, Tan Y, Liu L, Li S, Tan Z. Development of KASP markers, SNP fingerprinting and population genetic analysis of *Cymbidium ensifolium* (L.) Sw. germplasm resources in China. Front Plant Sci. 2025;15:1460603.
43. Tan Q, He H, Chen W, Huang L, Zhao D, Chen X, et al. Integrated genetic analysis of leaf blast resistance in upland rice: QTL mapping, bulked segregant analysis and transcriptome sequencing. AoB Plants. 2022;14:plac047.
44. Villa-Rodríguez E, Parra-Cota F, Castro-Longoria E, López-Cervantes J, Santos-Villalobos SD. *Bacillus subtilis* TE3: A promising biological control agent against *Bipolaris sorokiniana*, the causal agent of spot blotch in wheat (*Triticum turgidum* L. *subsp. durum*). Biol Control. 2019;132:135–43.
45. Wang R, Leng Y, Zhao M, Zhong S. Fine mapping of a dominant gene conferring resistance to spot blotch caused by a new pathotype of *Bipolaris sorokiniana* in barley. Theor Appl Genet. 2019;132:41–51.
46. Wang X, Mace ES, Platz GJ, Hunt CH, Hickey LT, Franckowiak JD, et al. Spot form of net blotch resistance in barley is under complex genetic control. Theor Appl Genet. 2015;128:489–99.
47. Williams KJ, Lichon A, Gianquitto P, Kretschmer JM, Karakousis A, Manning S, et al. Identification and mapping of a gene conferring resistance to the spot form of net blotch (*Pyrenophora teres* f *maculata*) in barley. Theor Appl Genet. 1999;99:323–7.

48. Yang G, Pan Y, Pan W, Song Q, Zhang R, Tong W, et al. Combined GWAS and eGWAS reveals the genetic basis underlying drought tolerance in emmer wheat (*Triticum turgidum* L). New Phytol. 2024;242:2115–31.
49. Ye J, Coulouris G, Zaretskaya I, Cutcutache I, Rozen S, Madden TL. Primer-BLAST: a tool to design target-specific primers for polymerase chain reaction. BMC Bioinf. 2012;13:134.
50. Yu D, Fan R, Zhang L, Xue P, Liao L, Hu M, et al. *HvWRKY2* acts as an immunity suppressor and targets *HvCEBiP* to regulate powdery mildew resistance in barley. Crop J. 2023;11:99–107.
51. Zhai H, Feng Z, Li J, Liu X, Xiao S, Ni Z, et al. QTL analysis of spike morphological traits and plant height in winter wheat (*Triticum aestivum* L.) using a high-density SNP and SSR-based linkage map. Front Plant Sci. 2016;7:1617.
52. Zheng C, Jiang Z, Meng Y, Yu J, Yang X, Zhang H, et al. Construction of a high-density SSR genetic linkage map and identification of QTL for storage-root yield and dry-matter content in sweetpotato. Crop J. 2023;11:963–7.
53. Zhou H, Steffenson B. Genome-wide association mapping reveals genetic architecture of durable spot blotch resistance in US barley breeding germplasm. Mol Breed. 2013;32:139–54. https://doi.org/10.1007/s11032-013-9858-4.
54. Zhu S, Liu C, Gong S, Chen Z, Chen R, Liu T, et al. Orthologous genes *Pm12* and *Pm21* from two wild relatives of wheat show evolutionary conservation but divergent powdery mildew resistance. Plant Commun. 2023;4:100472.

Table 1

Table 1
QTLs for leaf spot resistance in the barley RIL population

QTL	Chr	Interval	LOD	Phenotypic variance explained, PVE (%)	Additive effect
qSRH7-59	7	SNP-13635562 - SNP-27673224	3.25 ~ 3.35	0.02 ~ 1.14	-0.43~ -0.42
qSRH7-60	7	SNP-22554114 - SNP-27673224	3.25 ~ 3.53	0.02 ~ 2.28	-0.43~ -0.38
qSSH4-11	4	GBM1482-GMS089	3.33	7.39	-0.32
qSRH7-7	7	Bmg228-Bmg385	11.33	11.27	0.71
qSRH7-8	7	Bmg385-Bmg240	9.29	10.41	0.67
qSSH7-9	7	Bmg672-Bmg670	4.66	7.87	-0.58

Figures

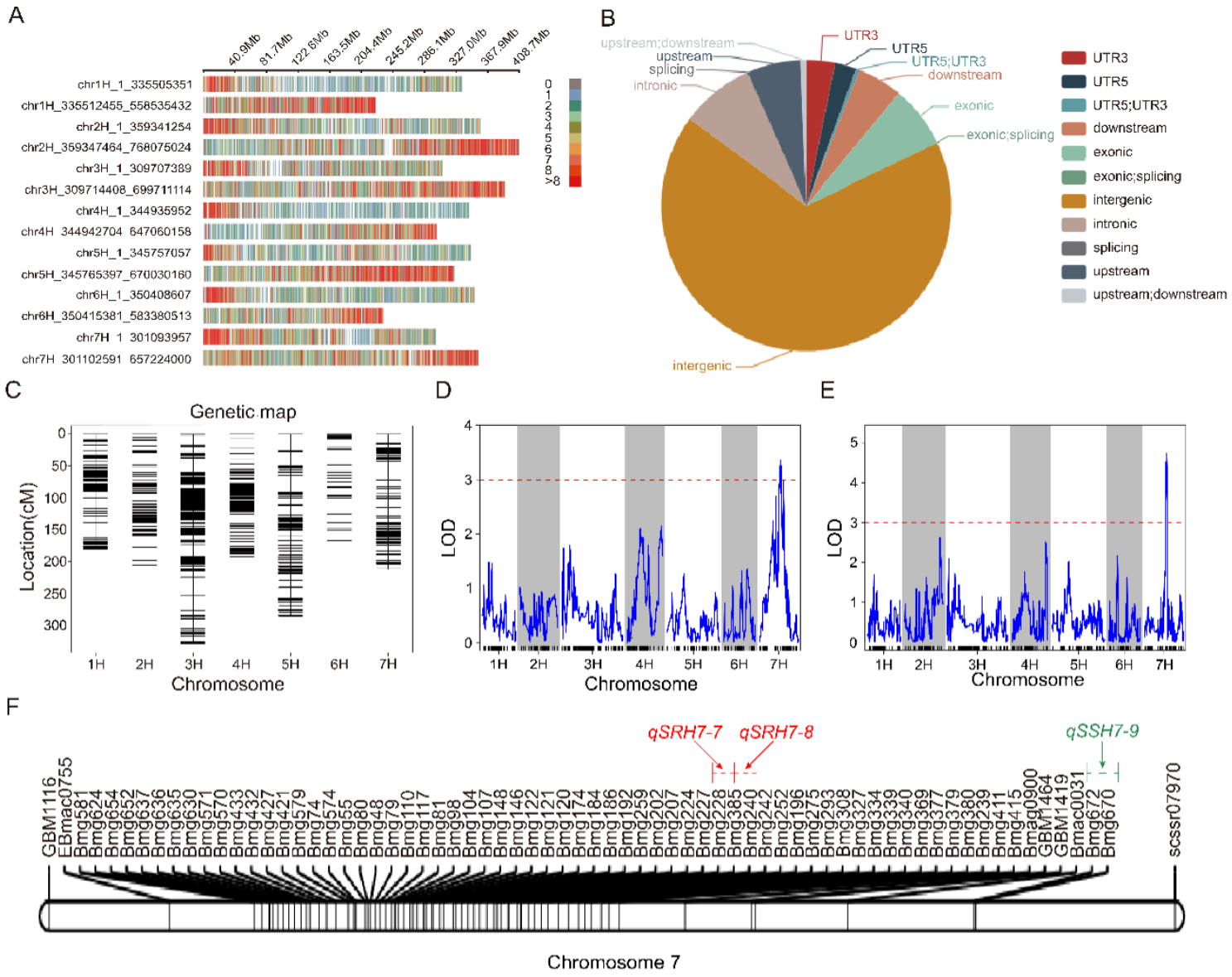

Figure 1

Comprehensive analysis of genetic markers and their distribution in the barley RIL population. (A) Physical distribution density of filtered SNPs in the RIL population, color gradient indicates marker density. (B) Annotation statistics of SNPs, UTR3: The mutation is located in the UTR region of the 3' end of the gene; UTR5: The mutation is located in the 5' UTR region of the gene; UTR5; UTR3: Mutations are located in the 5' UTR region and 3' UTR region of the gene; Downstream: Mutation located 2 Kb downstream of the gene; Exonic: The variation is located in the exon coding region; Exonic; Splicing: Mutations are located in exon coding regions and splicing sites; Intergenic: Variation is located in the intergenic region; Intronic: Variation is located in intron region; Upstream: mutation is located 2 Kb upstream of the gene; Upstream; Downstream: the mutation is located 2 Kb upstream and 2 Kb downstream of the gene. (C) Construction of a genetic linkage map based on SNP markers. (D) and (E) is LOD score profiles for QTL detection. Genetic positions (cM) are shown on the x-axis (chromosomes/linkage groups), with LOD scores on the y-axis. The blue line represents LOD score profiles. Vertical ticks below the blue line indicate marker positions. The red dashed line denotes the

significance threshold. (D) Interval mapping results; (E) Composite interval mapping results. (F) Chromosomal localization of QTLs conferring resistance to leaf spot disease on barley chromosome 7H, derived from a RIL population and an SSR-based genetic map. Red and green labels denote QTLs with positive and negative additive effects, respectively.

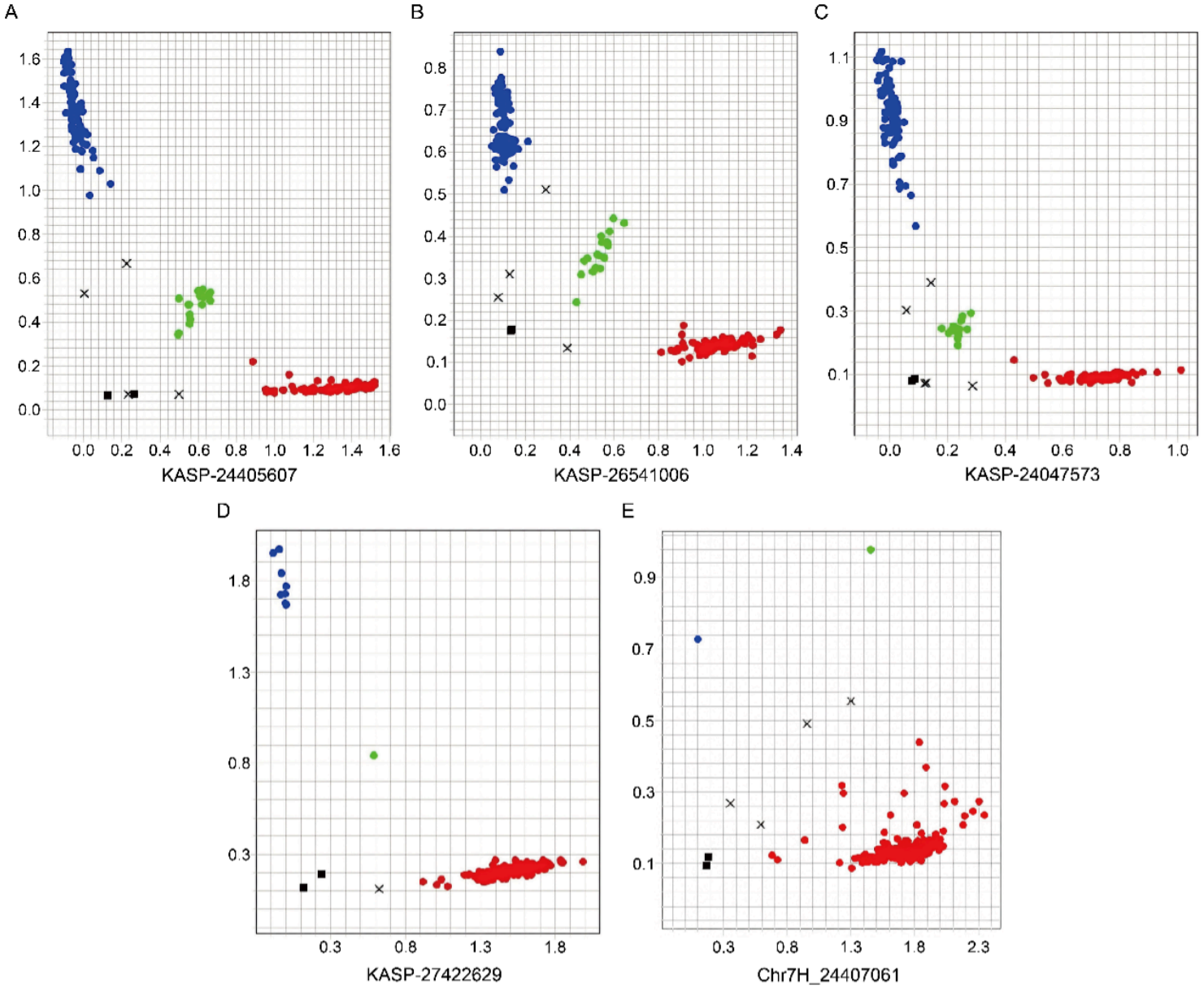

Figure 2

Genotyping plots of five KASP markers across 183 RILs. The genotyping results are clustered such that disease-resistant genotypes, identical to those of the parent cultivar MP3, are aggregated along the X-axis, while susceptible genotypes, identical to those of the parent cultivar MP1, are aggregated along the Y-axis. Blue dots represent individuals carrying the susceptible allele group; red dots represent individuals with the resistant allele group; and green dots indicate individuals with heterozygous alleles.

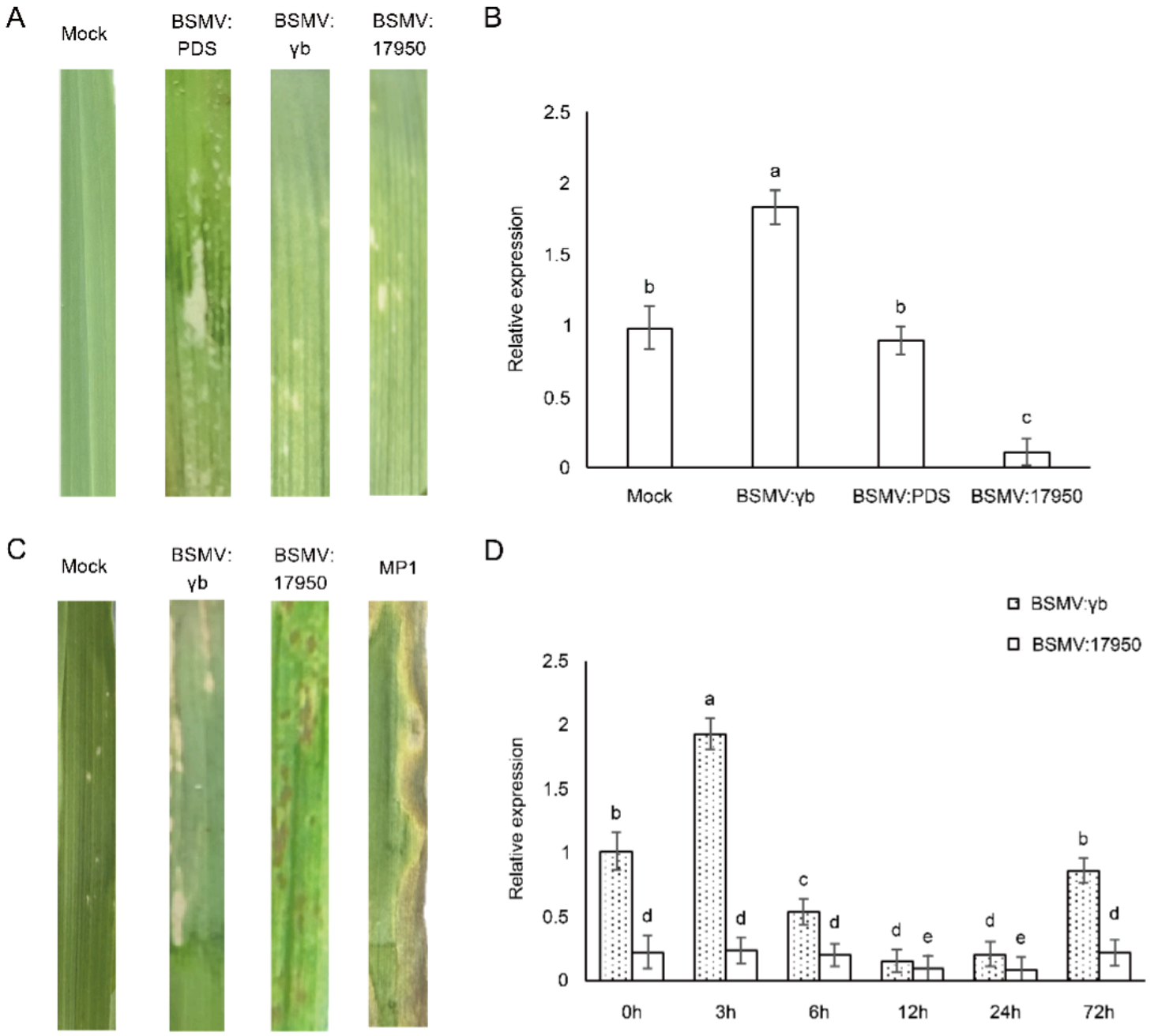

Figure 3

VIGS-based validation of *Hv7H.17950*. (A) New leaves of MP3 plants exhibiting varying degrees of photobleaching 14 days after inoculation with BSMV: PDS, BSMV: *Hv7H.17950*, and BSMV: γb on the first leaf. The BSMV-based VIGS system was used to assess gene silencing efficiency. (B) Relative expression levels of *Hv7H.17950*in leaf tissues treated with BSMV: PDS, BSMV: *Hv7H.17950*, BSMV: γb, or Mock (infiltrated with potassium phosphate buffer). Different lowercase letters indicate statistically significant differences among treatments at $P < 0.05$. (C) Disease phenotypes of MP3 (resistant genotype) 14 days after inoculation with the barley spot blotch pathogen *B. sorokiniana* strain Z14487, following the VIGS treatments shown in (A). MP1 inoculated with Z14487 for 14 days is shown as a susceptible with disease severity grade 6, confirming successful infection and experimental validity. (D) Expression dynamics of *Hv7H.17950*in MP3 plants pre-inoculated with either the BSMV: γb empty vector

and BSMV: *Hv7H.17950*, at 0 h, 3 h, 6 h, 12 h, 24 h, and 72 h after challenge inoculation with Z14487. Different lowercase letters indicate significant differences among treatments (P < 0.05).

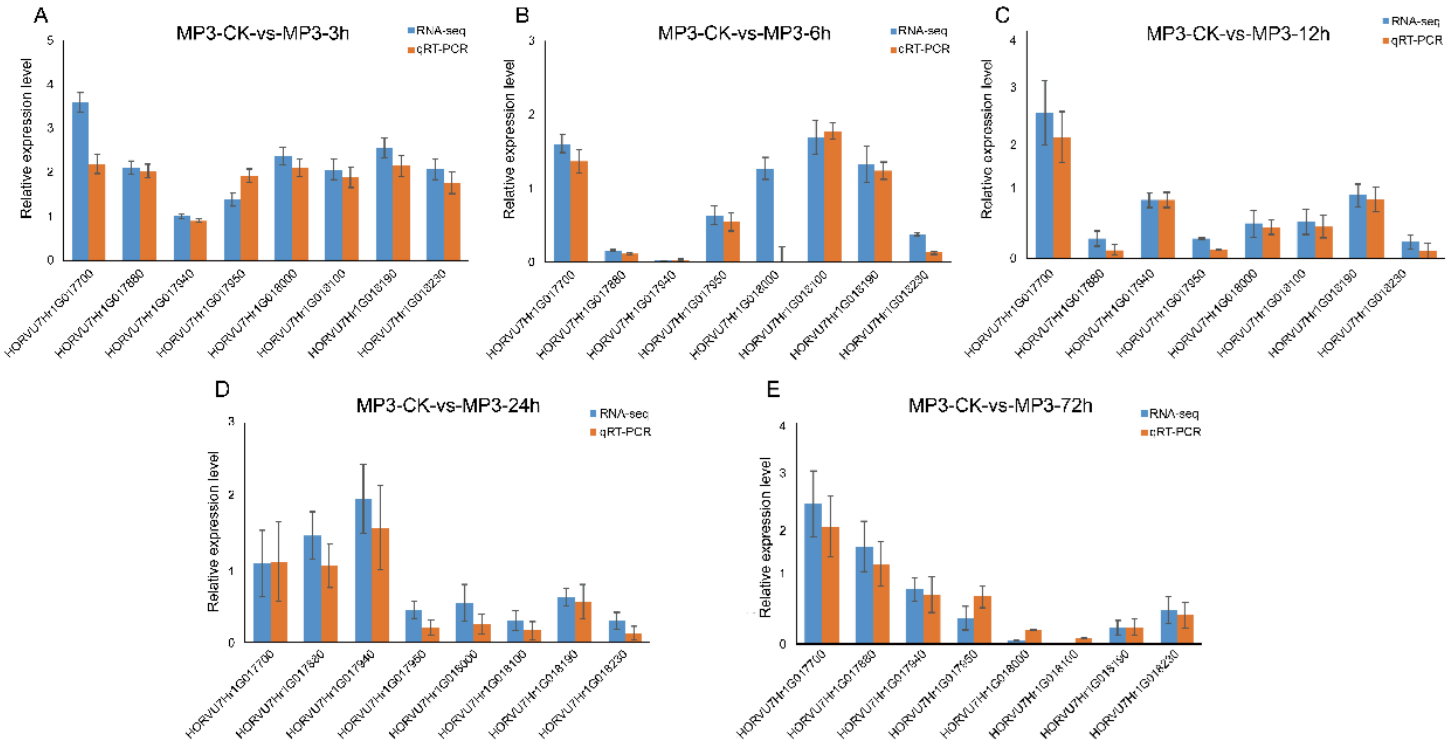

Figure 4

qPCR validation of candidate genes for spot blotch resistance in barley. (A) Relative expression levels of eight candidate genes at 3 hpi; (B) 6 hpi; (C) 12 hpi; (D) 24 hpi; (E) 72 hpi.

Supplementary Files

This is a list of supplementary files associated with this preprint. Click to download.

- Additionalfile1.docx
- Additionalfile2.xls